Arabian Journal of Geosciences (2022) 15: 1149
https://doi.org/10.1007/s12517-022-10337-6

ORIGINAL PAPER

Bamboo geocell for prevention of heavy rainfall-induced soil slope failure

Vamsiraju Adimilli[1] · Venkata Rama Subba Rao Godavarthi[1]

Received: 31 July 2020 / Accepted: 17 May 2022 / Published online: 10 June 2022

Abstract
Slope failures due to heavy rainfall are likely to occur during or after a certain period of rainfall. The present study aims at finding the possible soil slope failures when the slopes of different angles were exposed to heavy rainfall. Slopes of 30, 45, and 60° were made in a model test tank. It was found that the 60° slope was highly prone to failure in the event of heavy rainfall. Further, the present investigation aims at improving the 60° slope by reinforcing it with a low-cost natural geocell (bamboo geocell). Bamboo geocell of 50-mm thickness was covered on the surface of the 60° slope. It was evident that the 60° slope was protected with bamboo geocell has revealed no visible failure after exposure to a prolonged period of about 13 h of heavy rainfall.

Keywords Slope failure · Embankment · Heavy rainfall · Natural geocell · Bamboo geocell

Introduction

Slope failures are common geotechnical hazards in many places. Slope failures due to rainfall were evident in both natural and man-made slopes. Cut-slope and embankment slope have the potential to be prone to rainfall-induced slope failures. Failure of slope can happen in a matter of seconds during continued heavy rain. Heavy rainfall occurrences were projected as a result of climate change. During heavy rainfall, the water is found to flow along the surface of the slope. Rain is the predominant agent of surface soil erosion. Many slope failures were caused by infiltration of water, which induces an increase in pore-water pressure and seepage force in soil. In the period of rainfall and or subsequent time-lapse, the effective stress of the soil gets reduced owing to an increase in pore water pressure, which leads to reduction of shear strength and eventually leads to slope failure (Chueasamat et al. 2018; Askarinejad et al. 2018; Kluger et al. 2020; Cuomo, 2020; Dhanai et al. 2022). Because of the practical importance of the issue, understanding the slope stability has acclaimed the attention of civil engineers, especially geotechnical engineers, all around the world. Research in the area of slope stability as a result of rainfall infiltration was erstwhile carried out (Kristo, et al. 2017; Yao et al. 2019; Ghani et al. 2020). Slope failures can affect human lives and property loss. Vegetation along the slope can control the slope failures (Islam et al. 2020; Hu et al. 2018).

A new development in enhancing slope stability is by providing three-dimensional inclusion using geocell mattresses. Geocell mattress consists of a series of interlocking cells that can efficiently confine the soil within its cells. The geocell reinforcement can act as a beam that can carry both bending and membrane (Mehdipour et al. 2017). Geocells offer more rapid, economical, and sustainable solutions to many difficult geotechnical problems. Geocells were used in the construction of road, rail, and canal embankments and retaining structures (Venkateswarlu and Hegde 2019; Sitharam et al. 2020). Bamboo is a less expensive, environmentally friendly material, and it has higher tensile strength. The objective of the present investigation was to know the influence of heavy rainfall events on compacted soil slopes. Three model slopes of 30, 45, and 60° were made and exposed to heavy rainfall using an artificial rainfall simulation system. The rainfall simulator was capable of creating uniform drops and desired intensity. A rainfall simulator was planned to

Responsible Editor: Zeynal Abiddin Erguler

✉ Venkata Rama Subba Rao Godavarthi
gvramasubbarao@gmail.com

[1] Department of Civil Engineering, Velagapudi Ramakrishna Siddhartha Engineering College, Kanuru, Vijayawada, Andhra Pradesh 520 007, India

concern expected rain over the entire area of the compacted soil slope. The current study proposed to expose slopes to extreme rainfall intensity of about 8 mm/h. In this investigation, an attempt has been made to protect the surface of the steep slope (60°) against heavy rainfall. As a part of it, a natural geocell made of bamboo with 50-mm thickness was placed on the surface of the 60° slope. Rainfall can make the bamboo more prone to deterioration; therefore, it must be properly treated and prepared before use. Bamboo is treated with paints and varnishes to protect it from moisture and reduce biodegradability (NMBA 2006).

Materials and testing methodology

The soil used in the present study was collected from Kondaparva Village near Nuzvid Town (shown in Fig. 1) in the Krishna district of the Indian state of Andhra Pradesh. The grain size distribution of the soil was depicted in Fig. 2. The soil was classified as clayey sand of intermediate compressibility (SC-CI) based on the Unified Soil Classification System (ASTM D2487—17). The properties of the soil used in the present investigation were presented in Table 1. The bamboo used for making bamboo geocell has been collected from the Koyyalagudem region in Andhra Pradesh state, India. The bamboo strips of 50-mm width were used for making geocell (Fig. 3) and were used for making bamboo geocells. Oil varnish was applied on the surface of the bamboo strip, and it has long-time durability in order to protect bamboo from fungal and insect attacks. Treated bamboo has a tensile strength of 7.2 kN/m, whereas untreated bamboo has a tensile strength of 6.1 kN/m. The properties

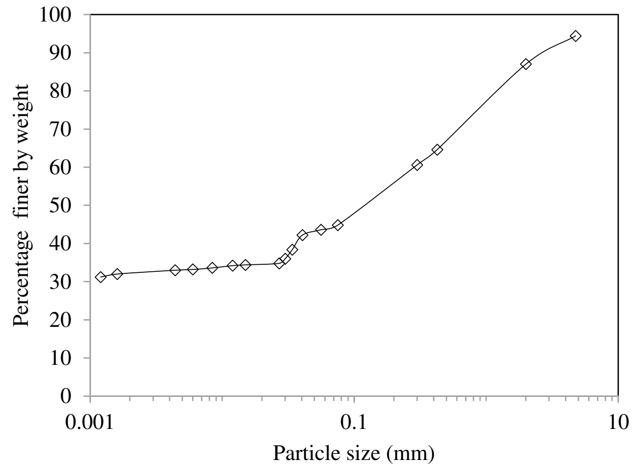

Fig. 2 Grain size distribution of soil

Fig. 1 Location of the collected soil-Kondaparva, near Nuzvid.

Table 1 Properties of the collected soil

Property	Value
Specific gravity	2.69
Gravel (%)	5.60
Sand (%)	49.60
Silt (%)	32.50
Clay (%)	12.30
Liquid limit (%)	47.00
Plastic limit (%)	19.48
Plasticity index (%)	27.52
Classification of soil (USCS)	SC-CI
Differential free swell index (%)	10.00
Degree of expansivity	Low
Modified compaction characteristics:	
Maximum dry density, MDD (g/cc)	2.032
Optimum moisture content, OMC (%)	10.5

Fig. 3 Bamboo geostrip

Table 2 Properties of the bamboo strip

Parameter	Value
Rib thickness (mm)	0.6
Node (junction) thickness (mm) [ASTM D5199—12]	3.2
Mass per unit area (gsm) [ASTM D5261—10]	901.9
Percent open area (%)	8.8
Tensile strength (kN/m) [ASTM D6241—14]	7.2

of the bamboo strip were presented in Table 2. The treated bamboo strips were folded in such a way that the aperture of the geocell was in the shape of an equilateral triangle having a side length of 50 mm. Bamboo strips were joined together using galvanized wire to make geocells. A closer view of bamboo geocell was presented in Fig. 4.

A model test tank has been fabricated to carry out the tests. The test tank was made up of iron and a supporting steel frame fixing the rainfall simulator on top of the model test tank. The width of the embankment slope was equal to the width of the test tank. The tank has an inner dimension of 1.60 m × 0.55 m in plan and a height of 1 m. Fiber-glass walls having a thickness of 12 mm were fixed along the length of the tank. A gravel layer of 0.10-m thickness was placed over the base of the tank, which acts as a drainage layer (Fig. 5). A jute woven geotextile (Fig. 6) was placed between the base of the slope and the drainage layer. The test setup was presented in a schematic diagram (Fig. 7) which shows the location of the drainage layer, drainage outlet, separator, soil slope, bamboo geocell, and rainfall simulator. An experimental investigation has been carried out to understand systematically the mechanism of slope failure due to heavy rainfall. A video camera was placed in front of the slope face to get a clearer view of the failure.

Fig. 4 Bamboo geocell

Fig. 5 Laying of drainage layer (gravel layer)

The soil was air-dried and pulverized with a tamping rod and passed through 4.75 mm. The soil was thoroughly mixed with the required quantity of water which is equal to the optimum moisture content (10.02%) and then the soil inside the tank was compacted with its respective maximum dry density (2.032 g/cc). A static roller of weight 37 kg with a number of passes of 100 was used to achieve the desired

Fig. 6 Placing of jute geotextile as a separator between drainage layer and soil

maximum dry density. The density of compacted soil was controlled by collecting soil cores. Transparent plastic stickers were marked on the side of the tank (on glass) to mark the slope line. The rainfall simulator (as shown in Fig. 8) was developed by providing a series of showers. The rainfall intensity of 8 mm/h was maintained for all the tests carried out in this study. The rainfall duration was measured with the stopwatch.

Results and discussion

30° slope

Duration of rainfall for the 30° slope was carried out up to 757 min 0 s. From the digital image analysis (Fig. 9), it was observed that the majority of slope failure was found to be a rill erosion (Fig. 10). Rainfall is supposed to be the cause of soil erosion. Rill erosion happens once runoff water forms small channels as it moves down a slope. Rill erosion is the consequence of poor water infiltration into soil slope. When the slope was exposed to heavy rainfall for 100 min, the majority of rill erosion occurred. There was no visible failure in 30° slope even after prolonged period of heavy rainfall. Appropriate erosion mitigation strategies should be applied to reduce erosion risk. Unconfined compressive strength (UCS) tests were performed according to the procedure laid in ASTM D2166. UCS is one of the quick and useful tests for evaluating the strength characteristics of cohesive soils (Eslami and Akbarimehr 2021). UCS of the soil before slope failure was 68.5 kN/m^2. The UCS test was conducted on a soil sample collected from a 30° slope after being subjected to heavy rainfall for a duration of 757 min. The reduction in UCS due to heavy rainfall exposure was about 47%. A stress-strain plot of soil used for making a 30° slope (before and after slope failure) was depicted in Fig. 11. After the failure of soil due to the rainfall, the eroded soil was collected and weighed. The soil loss ratio is the ratio of soil loss weight to the total weight of compacted soil. Soil loss is caused by a sufficient volume of run-off to move particles, and this can be protected by the surface of the slope. The soil loss ratio is very low for 30° slope. The

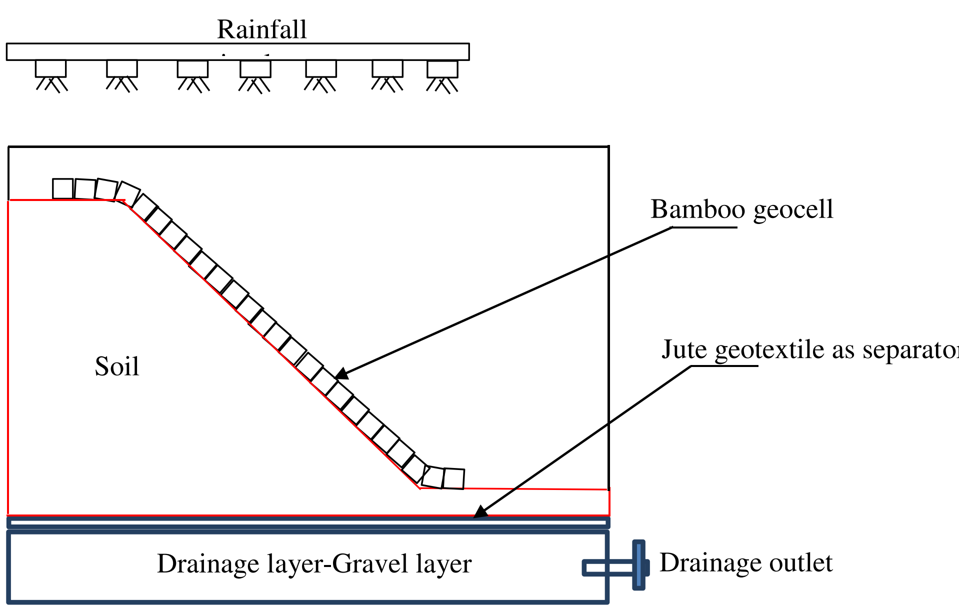

Fig. 7 Schematic diagram of the test set-up

Fig. 8 Rainfall simulator

soil loss ratio of the 30° slope was 3.57%. The surface and subsurface runoff water are collected and measured. Surface run-off is the most common cause of run-off during heavy rain events, and it can disturb soil structure and cause substantial soil loss. The surface runoff is collected in the tank using the outlet placed at 20 cm from the base of the test tank. The subsurface runoff was collected in the tank by using the outlet which has been placed at the bottom of the test tank. Surface and sub-surface volumes of water passed over and through 30° slope for different events of rainfall were presented in Table 3.

45° slope

UCS of 56.4 kN/m^2 was obtained on a soil sample collected from a 45° slope after being subjected to heavy rainfall for a duration of 702 min 20 s. Varied rainfall durations have different effects on the slope. The reduction in UCS was about 56.52%. A reduction in strength with an increase in slope angle is may be due to more reduction in matric suction at soil surface for the 45° slope as compared with the 30° slope. Due to an increase in pore water pressure, the effective pressure decreases, which in turn results in a reduction of shear strength of the soil. The effective stress in the soil will be decreased and thus reduces the soil shear strength, eventually resulting in slope failure. There was no further failure in the 45° slope after being exposed to a prolonged period of heavy rainfall (Fig. 12). It was noticed that the slope failure transformed from rill to non-circular rotational failure (Fig. 13). After the soil failure, the eroded soil was collected and weighed. The soil loss ratio of this slope was 2.89%. The exposure of the slope to heavy rainfall is the major factor controlling the soil loss by water. Surface and subsurface runoff water was collected and measured. The subsurface runoff was collected in the tank, with an outlet placed at the bottom of the test tank. Surface and sub-surface volumes of water passed over and through 45° slope for different events of rainfall were presented in Table 4. Excess pore water pressure may be the key source of slope instability.

60° slope

For a 60° slope as shown in Fig. 14, erosion immediately starts after commencement of rainfall exposure. Significant erosion of slope failure occurs after rainfall duration of 200 min; a clear circular-rotational failure was noticed at the top of the slope (Fig. 15). The 60° slope was highly susceptible to failure within the short duration of heavy rainfall. UCS value of 24.47 kN/m^2 was obtained for soil sample collected from 60° slope after being subjected to heavy rainfall for a duration of 211 min 52 s. Increased pore water pressure reduces the effective stress and shear strength of soil, lowering the UCS. Rainfall duration is the most significant aspect in determining whether slopes will fail or not. The percentage reduction in UCS is about 81.2%. It was observed that the 60° slope showed a high soil loss ratio when compared to the 30° and 45° slopes. Slope failure depends on the angle of the slope. The angle of the slope has an enormous effect on slope failure. The details of slope failure varied with each experiment. The soil loss ratio of this slope is 5.01%. The erosion effect was larger, and soil loss was greater as the slope angle increased. Surface and sub-surface volume of water passed over and through 60° slope for different events of rainfall were presented in Table 5. As the slope angle increases, the depth of surface erosion increases, due to faster flowing surface run-off. High water infiltration is caused by increased pore water pressure. Rainwater infiltrates into the soil and diminishes cohesion. Heavy rains caused the majority of slope failures by causing unsaturated sediments to lose their apparent cohesiveness. Active sliding is caused by water erosion during heavy rains. The shear strength of soil slope gets reduced when cracks were present. Water-filled cracks also lead to the development of extra driving forces. Regardless of how long rainfall continues, it was observed that the volume of subsurface water collected was 70 to 80% less than surface water. The speed of runoff accelerates on 60° slope, which increases the tendency of water to break off and transport soil particles. Over time, the soil deteriorates and becomes thinner with rainfall. Once, the slope tapers off and fattens at the base.

Protecting the 60° slope with bamboo geocell

The slope performance was well improved by the new bamboo geocell system. Bamboo is a biodegradable material that is commonly used to stabilize temporary slopes. Bamboo, on the other hand, may be made more durable and last for a long time with correct treatment and preparation.

Fig. 9. View of 30° slope at different durations of heavy rainfall. (**a**) 30° slope at 0 min 0 s, (**b**) 30° slope at 103 min 51 s, (**c**) 30° slope at 489 min 36 s, (**d**) 30° slope at 757 min 0 s

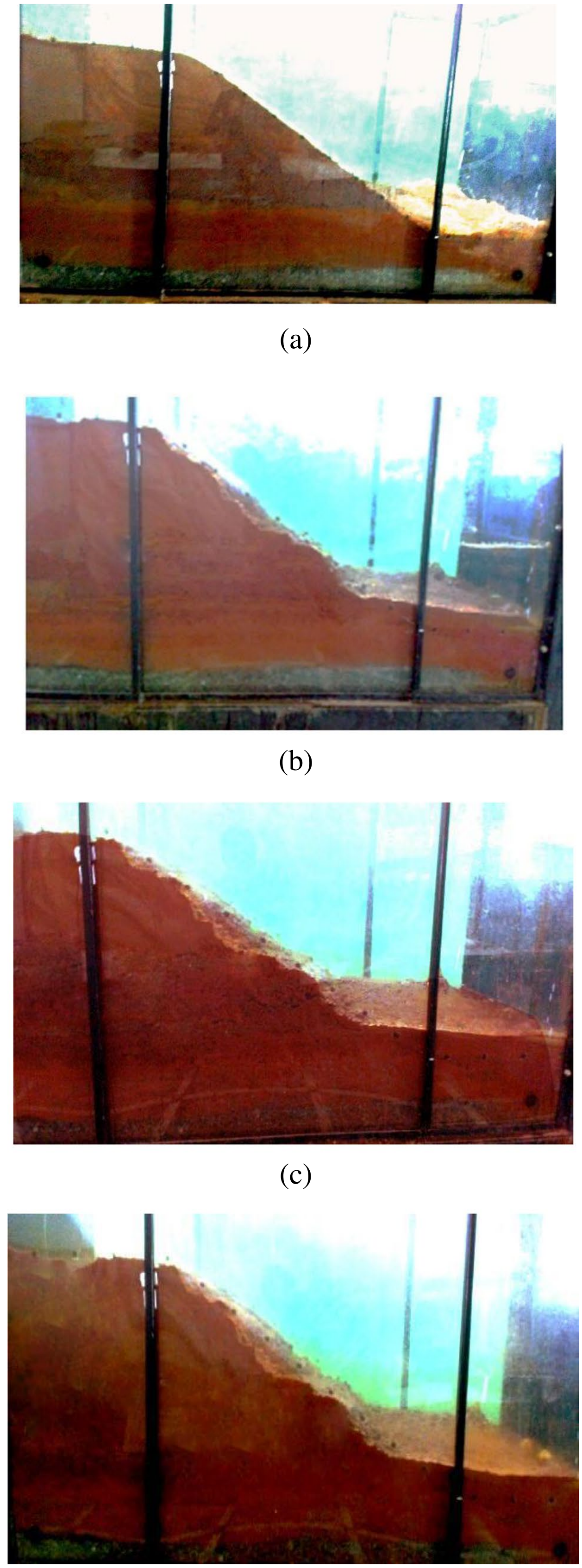

(a) (b) (c) (d)

The study was carried out on a sloped surface covered with and without bamboo geocell. Rainfall-induced slope failures can be prevented by using bamboo geocell as a reinforcement. Bamboo was used as natural reinforcement in the form of three-dimensional cells, which are similar to geocells. Bamboos were first cut into 20-mm-wide strips of a certain length, then braided together with galvanized wires to make a grid. Bamboo geocells were created by tying bamboo grids together. When the slope's topsoil needs to be protected from being washed away by rain, a bamboo geocell comes in handy. Plants will be able to grow on top of the bamboo geocell-protected slope as a result. Bamboo has been used as a soil stabilization reinforcement material (Gidon and Sahoo, 2020). Bamboo geocell can act as a natural roof for 60° slope which in turn significantly decreases run-off and soil erosion. Protecting the 60° slope against heavy rainfall becomes indispensable, and hence the present study was focusing on improving the 60° slope by placing bamboo geocell over the slope (shown in Fig. 16). U-pins of 14 cm in length were used to fix the bamboo geocell over the slope. After fixing the geocell on the slope, pockets of geocell were filled with soil and lightly compacted to avoid air voids in the bamboo geocell. Seeds were sown at 1-cm depth along the slope. The vegetation growth was observed in the period of 60 days (Fig. 17). Electric light was provided to simulate natural sunlight for ensuring plant growth by the process of photosynthesis. Any visible slope failure was not evident for a prolonged period of heavy rainfall, about 837 min (Fig. 18). It can be said that bamboo geocell can control erosion effectively even for long periods of rainfall events. Bamboo geocell can allow excellent growth of vegetation, and hence it offers more stability to the compacted steep slope (60° slope). UCS of the soil was 68.26 kN/m^2 obtained for the soil sample collected from this slope after being subjected to heavy rainfall for a duration of 837 min. It was observed the reduction in UCS was about 47.59%. Surface and sub-surface volume of water passed over and through bamboo geocell protected 60° slope for different events of rainfall was presented in Table 6.

Conclusions

The following conclusions can be drawn from the present study:

1. Digital image analysis has been carried out on the 30° slope, which was subjected to heavy rainfall for a dura-

Fig. 10 Rill erosion observed in 30° slope

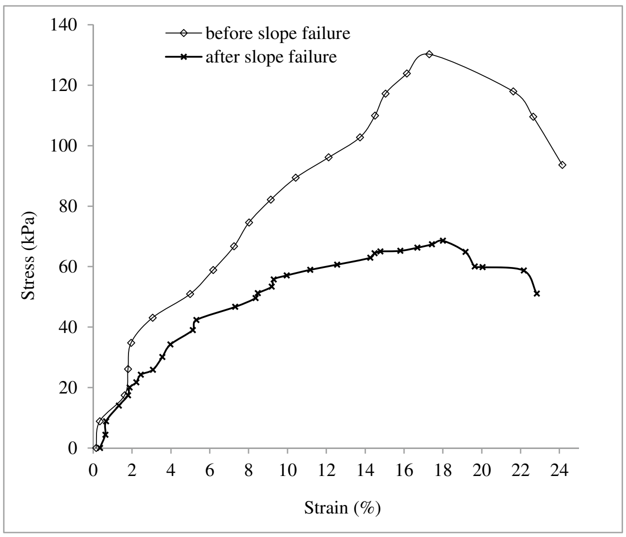

Fig. 11 Stress-strain behavior of the soil used for making 30° slope (Before and after slope failure)

Table 3 Surface and sub-surface volume of water passed over and through 30° slope

Rainfall event	Duration of rainfall (in min)	Volume of water collected (in cm^3)	
		Surface volume	Sub-surface volume
1	49.7	1,238,400.0	191,128.5
2	207.4	4,419,200.0	548,341.5
3	155.3	3,792,000.0	484,632.0
4	143.0	3,827,200.0	382,257.0
5	120.7	3,200,000.0	400,447.5
6	80.6	1,907,200.0	211,603.5
Total	757.0	18,380,000.0	2,218,410.0

tion of 757 min 0 s. It was found that the majority of slope failure is found to be rill erosion.

2. Unconfined compressive strength (UCS) of the soil collected from the surface of 30° slope which has been

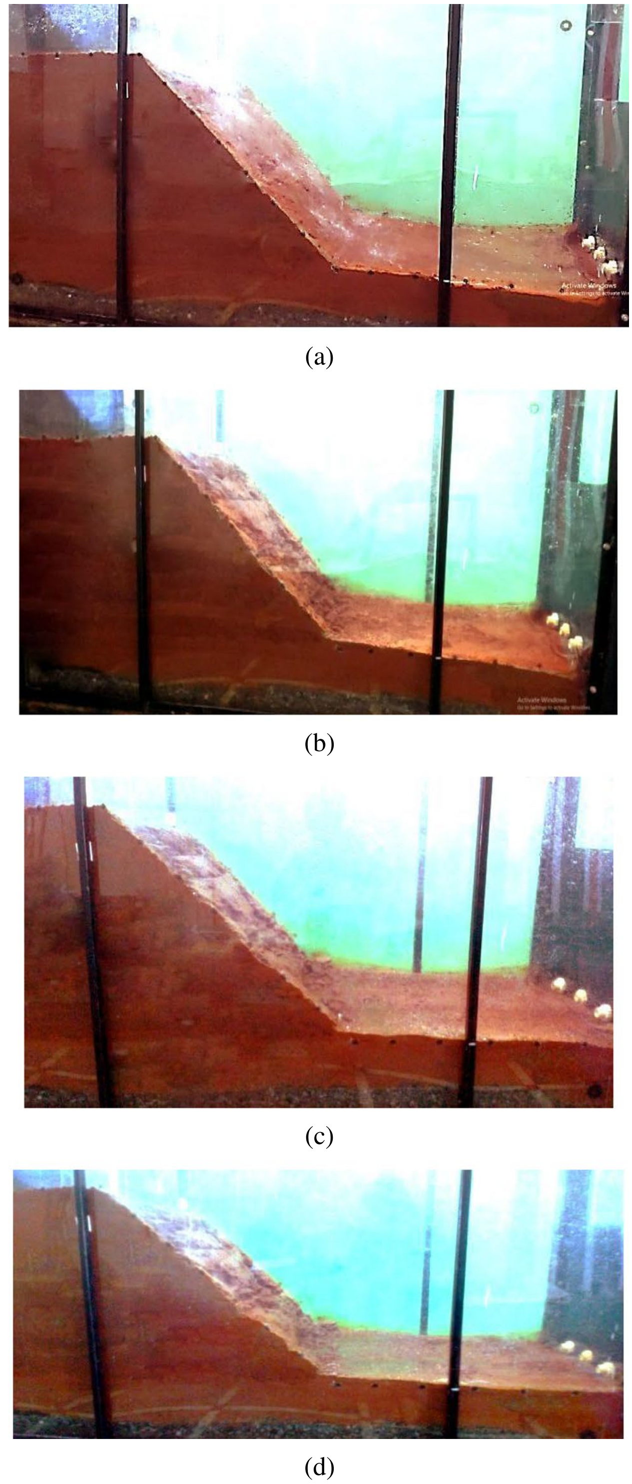

Fig. 12 View of 45° slope at different durations of heavy rainfall, (**a**) 45° slope at 0 min 0 s, (**b**) 45° slope at 220 min 51 s, (**c**) 45° slope at 422 min 37 s, (**d**) 45° slope at time 702 min 17 s

Fig. 13 Rill to non-circular rotational failure for 45° slope

Table 4 Surface and sub-surface volume of water passed over and through 45° slope

Rainfall event	Duration of rainfall (in minutes)	Volume of water collected (in cm^3)	
		Surface volume	Sub-surface volume
1	47.0	1,248,000.0	300,993.3
2	203.0	4,105,600.0	118,0631.2
3	172.6	3,702,400.0	943,927.5
4	168.4	3,747,200.0	987,750
5	111.2	2,464,000.0	558,168.7
Total	702.3	15,267,200.0	3,971,470.8

exposed to heavy rainfall shows a reduction in strength of about 47%. The soil loss ratio is very low and is 3.57% for the 30° slope.

3. Digital image analysis has been carried out on the 45° slope which was subjected to heavy rainfall for a duration of 702 min 20 s. It was found that the rill erosion took place more regularly as compared to the 30° slope. After 300 min, the slope failure transformed from rill erosion to non-circular rotational failure.
4. UCS of the soil collected from the surface of the 45° slope exposed to heavy rainfall shows a reduction in strength of about 56.52%. The soil loss ratio of this slope was 2.89%.
5. Digital image analysis has been carried out on a 60° slope showing that erosion starts immediately after commencement of exposure to heavy rainfall. Significant erosion of slope failure occurs after 200 min; a clear circular-rotational failure was noticed at the top of the slope.
6. UCS of the soil collected from the surface of the failed 60° slope shows a reduction in strength of about 81.2%. The saturation of soil slope due to the rainfall process

(a)

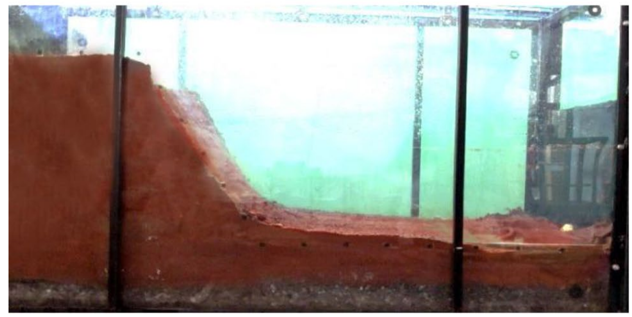

(b)

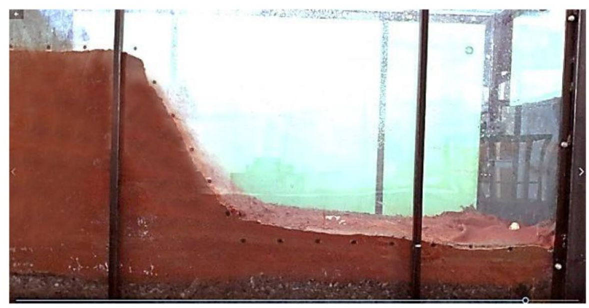

(c)

Fig. 14 View of 60° slope at different durations of heavy rainfall, (**a**) 60° slope at 0 min 0 s, (**b**) 60° slope at 47 min 36 s, (**c**) 60° slope at 211 min 52 s

Fig. 15 Circular-rotational failure for 60° slope

Table 5 Surface and sub-surface volume of water passed over and through 60° slope

Rainfall event	Duration of rainfall (in min)	Volume of water collected (in cm^3)	
		Surface volume	Sub-surface volume
1	48.6	116,721.0	200,115.0
2	57.5	1,184,000.0	170,640.0
3	47.6	1,129,600.0	150,165.0
4	58.1	1,200,000.0	150,165.0
Total	211.8	3,630,321.0	671,085.0

Fig. 16 Placing of bamboo geocell over compacted 60° slope

Fig. 17 Vegetation growth in the period of 60 days

significantly reduces the shear strength of the soil. It was observed that the 60° slope exhibits a high soil loss ratio, about 5.01% as compared to the 30 and 45° slopes. The maximum soil loss ratio in a short duration of rainfall occurs in the 60° slope.

7. 60° slope is highly prone to instability, especially for heavy rainfall of short duration. Therefore, protecting steep slopes against heavy rainfall was essential. Bamboo geocell was performed better for the protection of slope and also for erosion control.

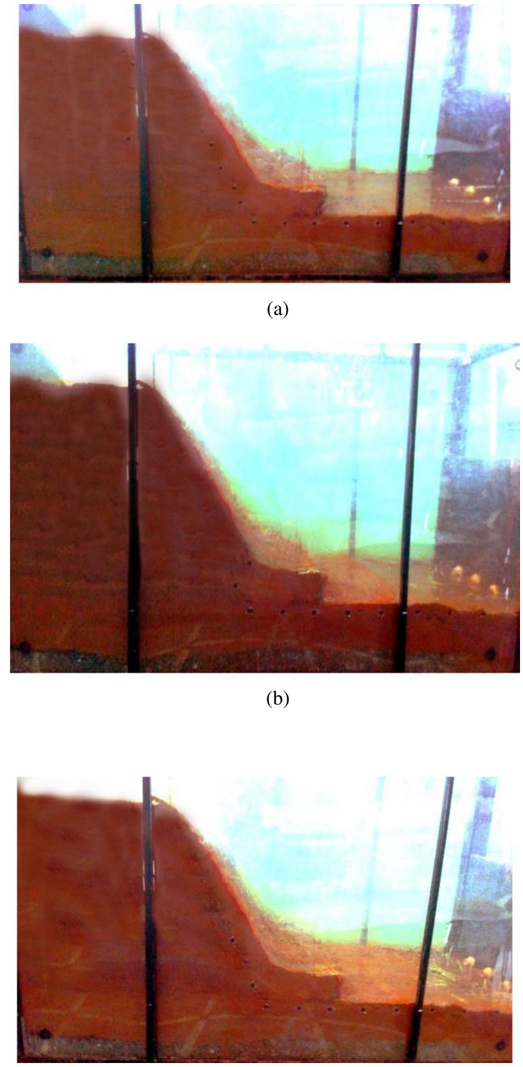

(a)

(b)

(c)

Fig. 18 View of bamboo geocell protected 60° slope at different durations of heavy rainfall, (**a**) Bamboo geocell protected 60° slope at 0 min 0 s, (**b**) Bamboo geocell protected 60° slope at 253 min 54 s, (**c**) Bamboo geocell protected 60° slope at 837 min 54 s

Table 6 Surface and sub-surface volume of water passed over and through bamboo geocell protected 60° slope

Rainfall event	Duration of rainfall (in min)	Volume of water collected (in cm^3)	
		Surface volume	Sub-surface volume
1	26.7	640,000.0	86,469.0
2	103.1	2,515,200.0	193,413.0
3	26.9	640,000.0	43,234.5
4	243.4	6,348,800.0	407,301.0
5	179.2	4,467,200.0	279,882.0
6	180.5	4,460,800.0	236,647.5
7	77.9	1,913,600.0	86,469.0
Total	837.0	19,072,000.0	1,246,947.0

Acknowledgements The authors were grateful to Prof. K. Mallikarjuna Rao, Department of Civil Engineering, Sri Venkateswara University College of Engineering, Tirupati, Andhra Pradesh, India for his constant motivation and guidance.

Declarations

Conflict of interest The authors declare no competing interests.

References

Askarinejad A, Akca D, Springman SM (2018) Precursors of instability in a natural slope due to rainfall: a full-scale experiment. Landslides 15:1745–1759. https://doi.org/10.1007/s10346-018-0994-0

ASTM D 2166 - 16 (2016) Standard test method for unconfined compressive strength of cohesive soil. ASTM International, West Conshohocken

ASTM D2487 – 17 (2017) Standard practice for classification of soils for engineering purposes (unified soil classification system). ASTM International, West Conshohocken

ASTM D5199 – 12 (2019) Standard test method for measuring the nominal thickness of geosynthetics. ASTM International, West Conshohocken

ASTM D5261 – 10 (2018) Standard test method for measuring mass per unit area of geotextiles. ASTM International, West Conshohocken

ASTM D6241 – 14 (2014) Standard test method for static puncture strength of geotextiles and geotextile-related products using a 50-mm probe. ASTM International, West Conshohocken

Chueasamat A, Hori T, Saito H, Sato T, Kohgo Y (2018) Experimental tests of slope failure due to rainfalls using 1g physical slope models. Soils and Foundations 58(2):290–305. https://doi.org/10.1016/j.sandf.2018.02.003

Cuomo S (2020) Modelling of flowslides and debris avalanches in natural and engineered slopes: a review. Geoenviron. Disasters 7(1). https://doi.org/10.1186/s40677-019-0133-9

Dhanai P, Singh VP, Soni P (2022) Rainfall triggered slope instability analysis with changing climate. Indian Geotech J. https://doi.org/10.1007/s40098-021-00581-0

Eslami A, Akbarimehr D (2021) Failure analysis of clay soil-rubber waste mixture as a sustainable construction material. Constr Build Mater 310. https://doi.org/10.1016/j.conbuildmat.2021.125274

Ghani ANC, Taib AM, Hasbollah DZA (2020) Effect of rainfall pattern on slope stability. In: Duc Long P., Dung N. (eds) Geotechnics for sustainable infrastructure development. Lecture Notes in Civil Engineering, vol 62. Springer, Singapore. https://doi.org/10.1007/978-981-15-2184-3_115

Gidon JS, Sahoo S (2020) Rainfall-induced slope failures and use of bamboo as a remedial measure: a review. Indian Geotech J 50:766–783. https://doi.org/10.1007/s40098-020-00409-3

Hu W, Scaringi G, Xu Q, Huang R (2018) Internal erosion controls failure and run out of loose granular deposits: evidence from flume tests and implications for post-seismic slope healing. Geophys Res Lett 45(11):5518–5527. https://doi.org/10.1029/2018GL078030

Islam MA, Islam MS, Elahi TE (2020) Effectiveness of vetiver grass on stabilizing hill slopes: a numerical approach. ASCE Geo-Congress 2020:106–115. https://doi.org/10.1061/9780784482797.011

Kluger MO, Jorat ME, Moon VG, Kreiter S, De Lange WP, Mörz T, Robertson T, Lowe DJ (2020) Rainfall threshold for initiating effective stress decrease and failure in weathered tephra slopes. Landslides 17:267–281. https://doi.org/10.1007/s10346-019-01289-2

Kristo C, Rahardjo H, Satyanaga A (2017) Effect of variations in rainfall intensity on slope stability in Singapore, International Soil and Water Conservation Research, Volume 5, Issue 4, Pages 258-264, ISSN 2095-6339, https://doi.org/10.1016/j.iswcr.2017.07.001

Mehdipour I, Ghazavi M, Reza Z (2017) Stability analysis of geocell-reinforced slopes using the limit equilibrium horizontal slice method. Intl J Geomech 17(9). https://doi.org/10.1061/(ASCE)GM.1943-5622.0000935

NMBA (2006) Preservation of bamboo-training manual, national mission on bamboo applications, technology information, forecasting, and assessment council (TIFAC), Department of science and technology, Government of India

Sitharam TG, Hegde AM Kolathayar S (2020) Geocells—advances and applications, https://link.springer.com/book/10.1007/978-981-15-6095-8

Venkateswarlu H, Hegde A (2019) Effect of infill materials on vibration isolation efficacy of geocell reinforced soil bed. Canadian Geotech J. https://doi.org/10.1139/cgj-2019-0135

Yao W, Li C, Zhan H et al (2019) Time-dependent slope stability during intense rainfall with stratified soil water content. Bull Eng Geol Environ 78:4805–4819. https://doi.org/10.1007/s10064-018-01437-3